

# Interface Reconstruction using Gaussian Processes for Volume of Fluid Methods



**Adam Reyes**

M. Adams, A. Armstrong<sup>1</sup>, K. Moczulski, P. Farmakis, E. Hansen, Y. Lu, D. Michta, P. Tzeferacos

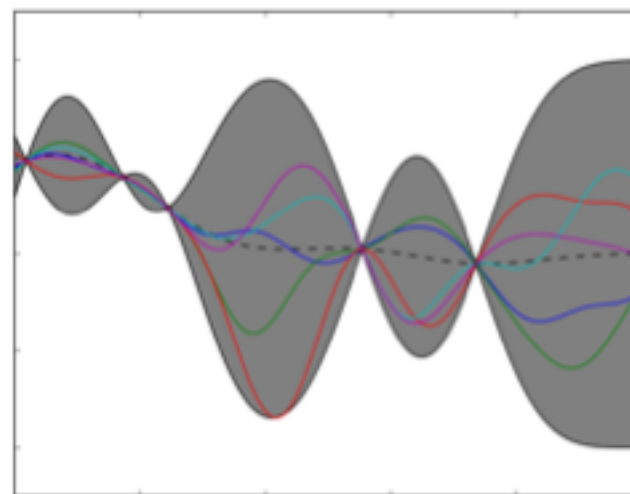
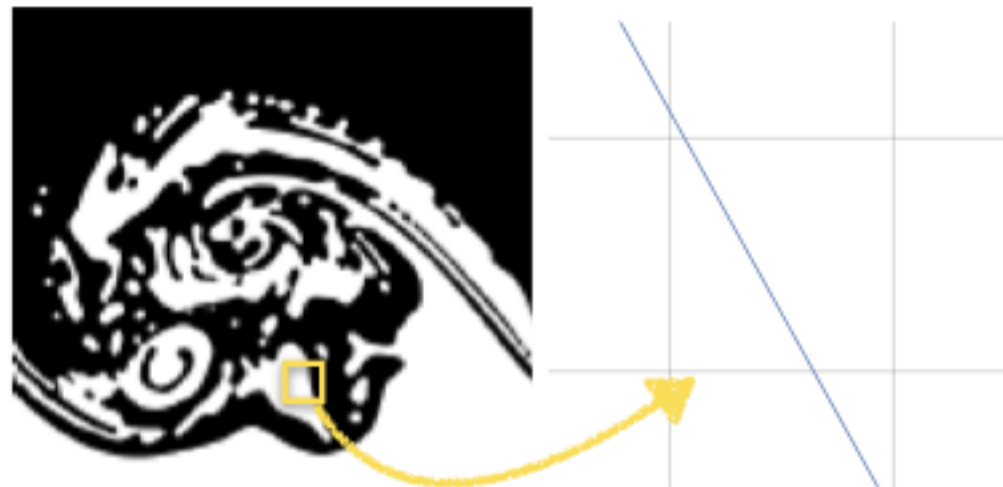
FLASH Center for Computational Science  
Department of Physics & Astronomy  
University of Rochester

64th Annual APS DPP  
Spokane, WA  
October 17, 2022



# Summary

- Volume of Fluid (VOF) methods combine conservation with sharp interface representation
  - Computationally efficient interface reconstruction algorithms that generalize to 3D can fail, even for simple linear interfaces
- Non-parametric Gaussian process function regression allows one to more accurately reconstruct interfaces, with the same computational cost





UNIVERSITY OF  
ROCHESTER



# Acknowledgments



Lawrence Livermore  
National Laboratory

The Flash Center acknowledges support by the U.S. DOE ARPA-E under Award DE-AR0001272, the National Science Foundation under Award PHY-2033925, and the U.S. DOE NNSA under Award DE-NA0003842, and Subcontracts 536203 and 630138 with LANL and B632670 with LLNL. This material is based upon work supported by the U.S. DOE NNSA under Award Number DE-NA0003856 through the Horton Fellowship Program at the Laboratory for Laser Energetics.

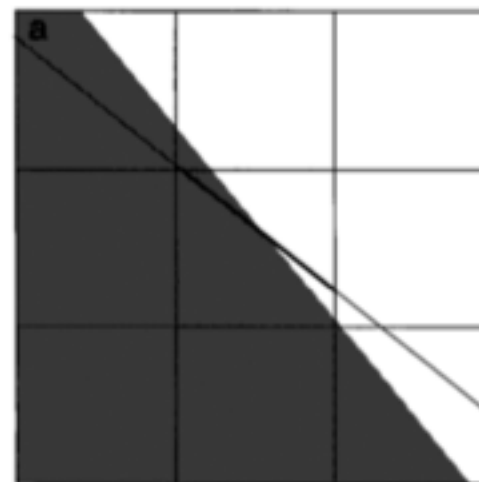
# Volume-of-Fluid

- Computational fluid dynamics (CFD) typically treated as an algebraic problem

$$U_i^{n+1} = U_i^n - \frac{1}{\Delta t} \int_{t^n}^{t^{n+1}} \frac{1}{\Delta x} (\hat{f}_{i+1/2} - \hat{f}_{i-1/2}) dt$$

- Tracking material interfaces is inherently a geometric problem
- The volume-of-fluid (VOF) method attempts to bridge the two
  - Evolve volume fraction of component fluids (interface capturing)
  - Reconstruct material interfaces from volume fractions

- Piecewise linear interface calculation (PLIC)
- Modified Youngs' method from Rider & Kothe looks for a Taylor polynomial that minimizes least-square residual of color function of on a 3x3 stencil
- Gradient yields interface normal
  - Line constant adjusted to match volume fraction



$$\mathbf{n} \cdot \mathbf{x} + \rho = 0$$

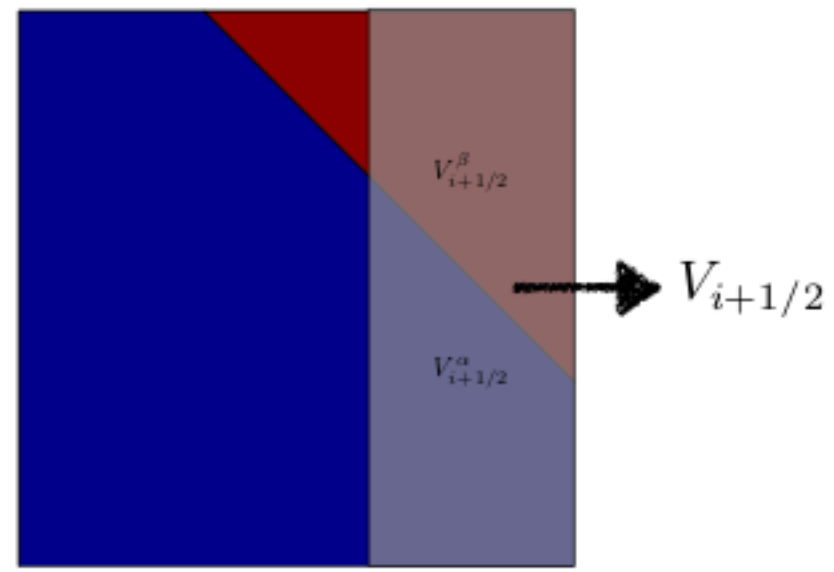
W. J. Rider and D. B. Kothe, "Reconstructing Volume Tracking," *Journal of Computational Physics*, vol. 141, no. 2, pp. 112–152, Apr. 1998, doi: [10.1006/jcph.1998.5906](https://doi.org/10.1006/jcph.1998.5906). [1]

D. Youngs, "An interface tracking method for a 3D Eulerian hydrodynamics code," Jan. 1984. [2]

T. J. Barth, "Aspects of Unstructured Grids and Finite-Volume Solvers for the Euler and Navier-Stokes Equations," Jan. 1994, Accessed: Jul. 10, 2019. [Online]. Available: <http://ntrs.nasa.gov/search.jsp?R=19960020994>. [3]

# Solution Update

- Calculate component advected volumes through normal faces



- Update fluid variables

$$f^\alpha \quad \rho^\alpha \quad e^\alpha$$

# Kelvin-Helmholtz Instability

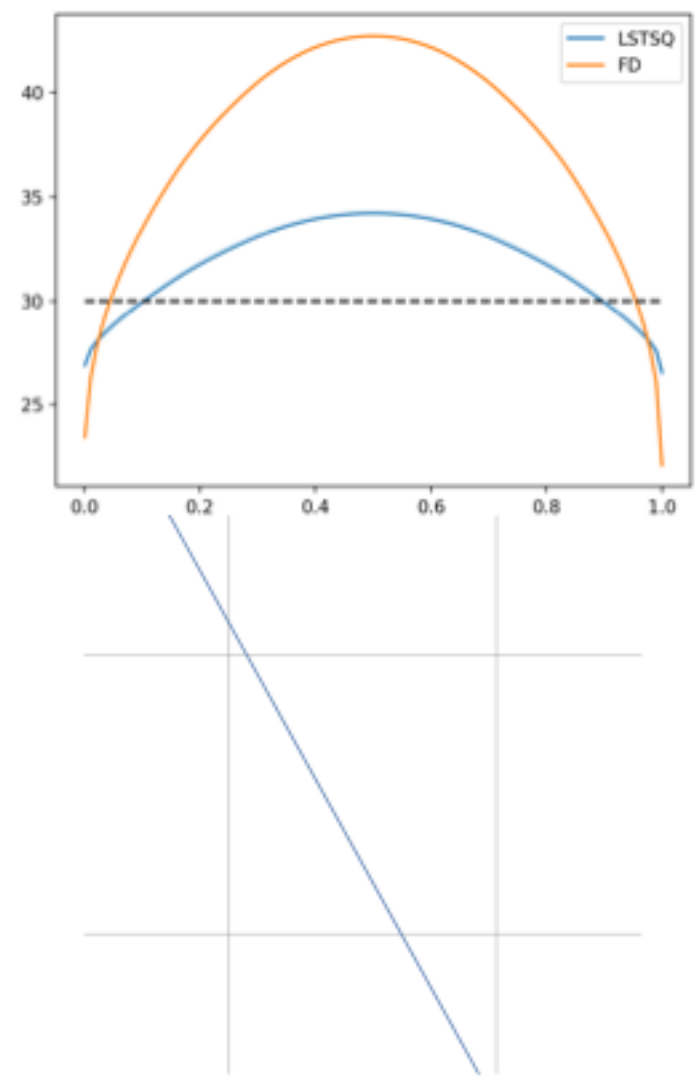


Time=0

# Interface Calculation

- Method is readily extended to 3D interfaces
- Can fail to perfectly reconstruct even linear interfaces
- Iterative methods can improve errors, but are prohibitively expensive in 3D

Reconstructed normal for 30° linear interface



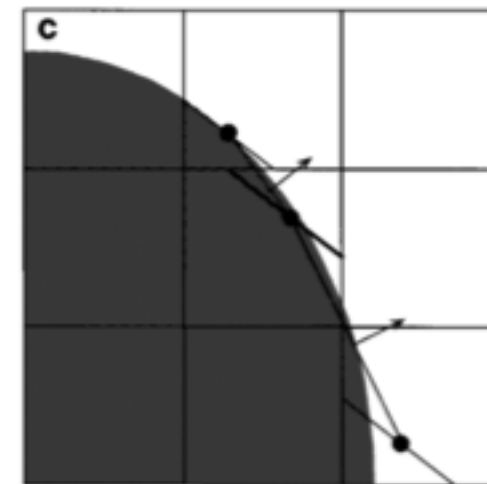
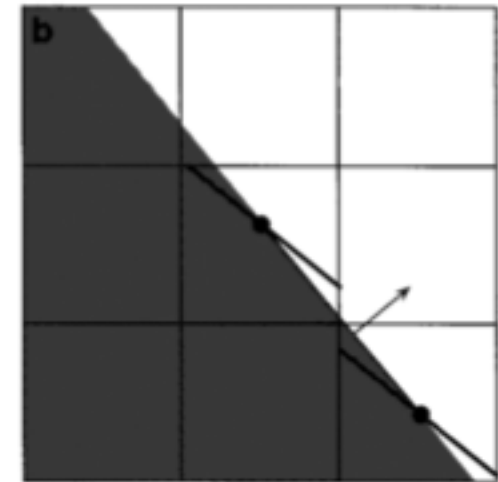
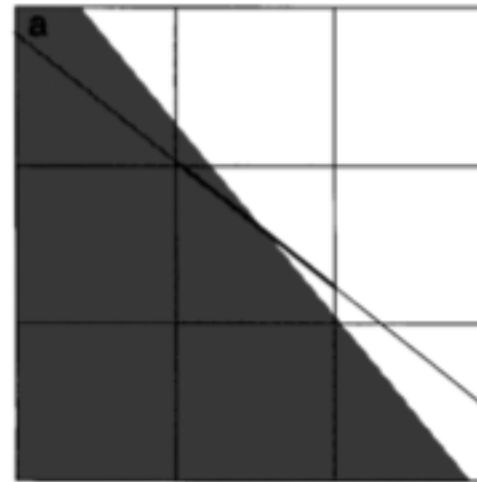
W. J. Rider and D. B. Kothe, "Reconstructing Volume Tracking," *Journal of Computational Physics*, vol. 141, no. 2, pp. 112–152, Apr. 1998, doi: [10.1006/jcph.1998.5906](https://doi.org/10.1006/jcph.1998.5906). [1]

D. Youngs, "An interface tracking method for a 3D Eulerian hydrodynamics code," Jan. 1984. [2]

T. J. Barth, "Aspects of Unstructured Grids and Finite-Volume Solvers for the Euler and Navier-Stokes Equations," Jan. 1994, Accessed: Jul. 10, 2019. [Online]. Available: <http://ntrs.nasa.gov/search.jsp?R=19960020994>. [3]



- Method is readily extended to 3D interfaces
- Can fail to perfectly reconstruct even linear interfaces
- Iterative methods can improve errors, but are prohibitively expensive in 3D



W. J. Rider and D. B. Kothe, "Reconstructing Volume Tracking," *Journal of Computational Physics*, vol. 141, no. 2, pp. 112–152, Apr. 1998, doi: [10.1006/jcph.1998.5906](https://doi.org/10.1006/jcph.1998.5906). [1]


D. Youngs, "An interface tracking method for a 3D Eulerian hydrodynamics code," Jan. 1984. [2]

T. J. Barth, "Aspects of Unstructured Grids and Finite-Volume Solvers for the Euler and Navier-Stokes Equations," Jan. 1994, Accessed: Jul. 10, 2019. [Online]. Available: <http://ntrs.nasa.gov/search.jsp?R=19960020994> [3]

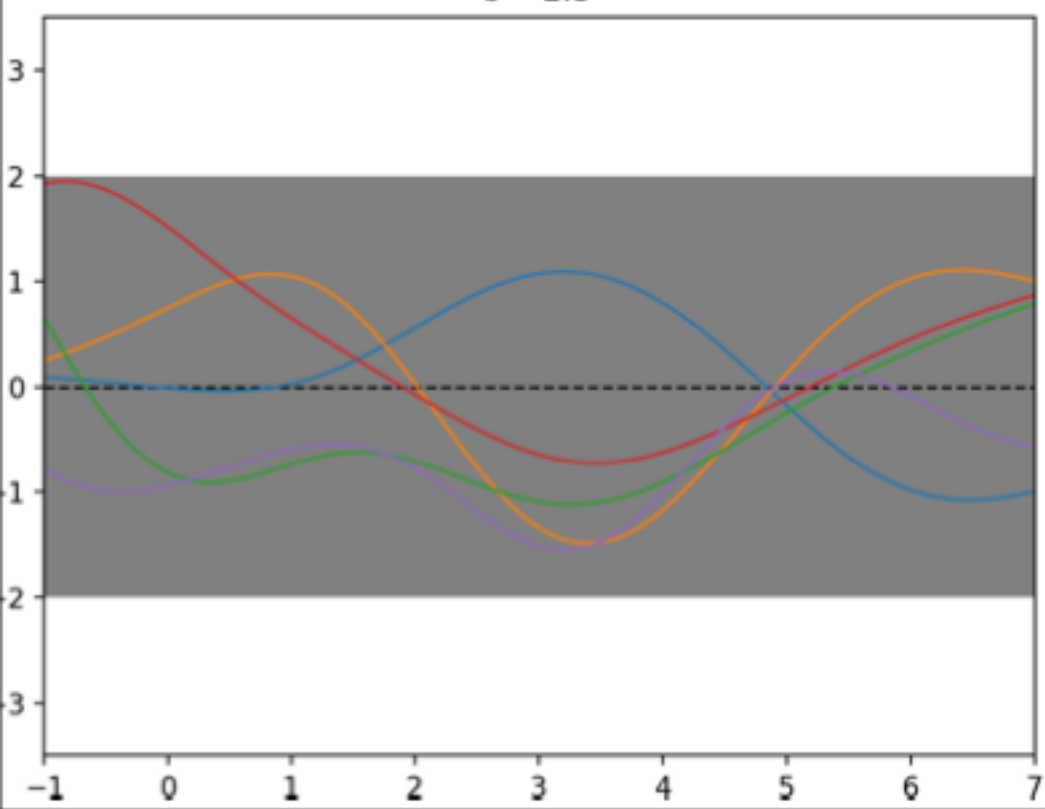
- View function values at points in space as having a joint Gaussian probability distribution

$$\mu(x) = 0$$

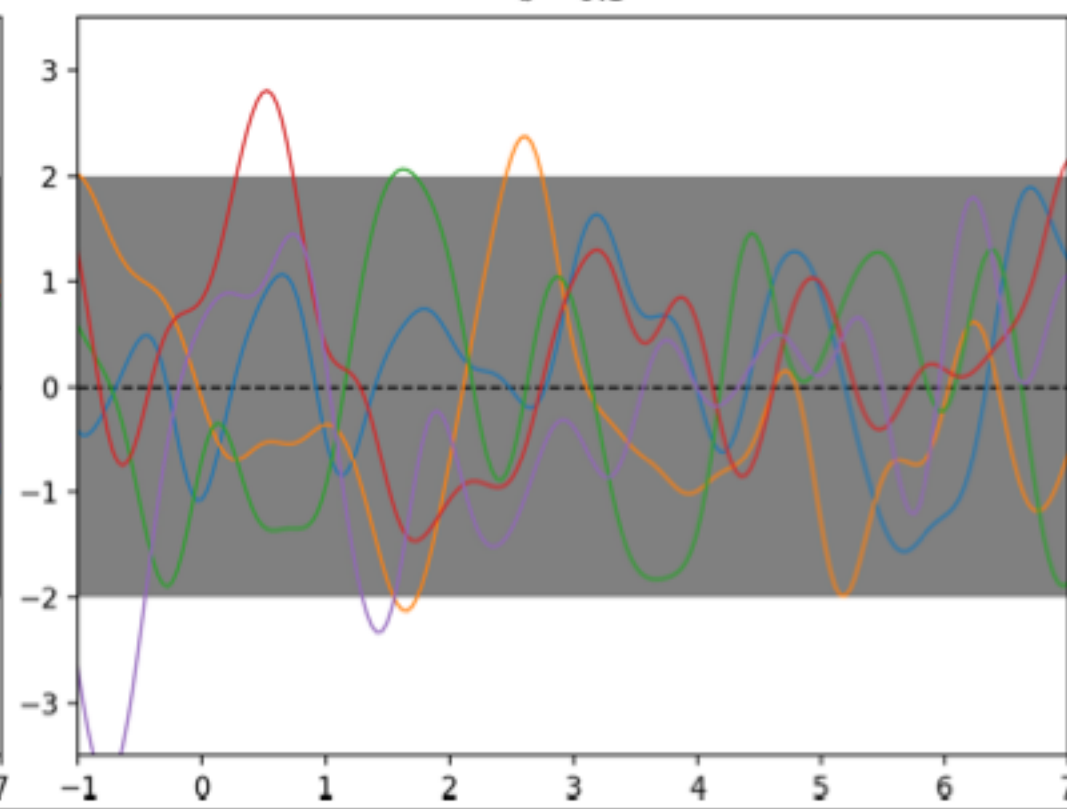
$$K_{SE}(x, y) = \exp \left[ -\frac{(x - y)^2}{2\ell^2} \right]$$

  
 Covariance between function values at different spatial locations

$\ell = 1.5$



$\ell = 0.3$

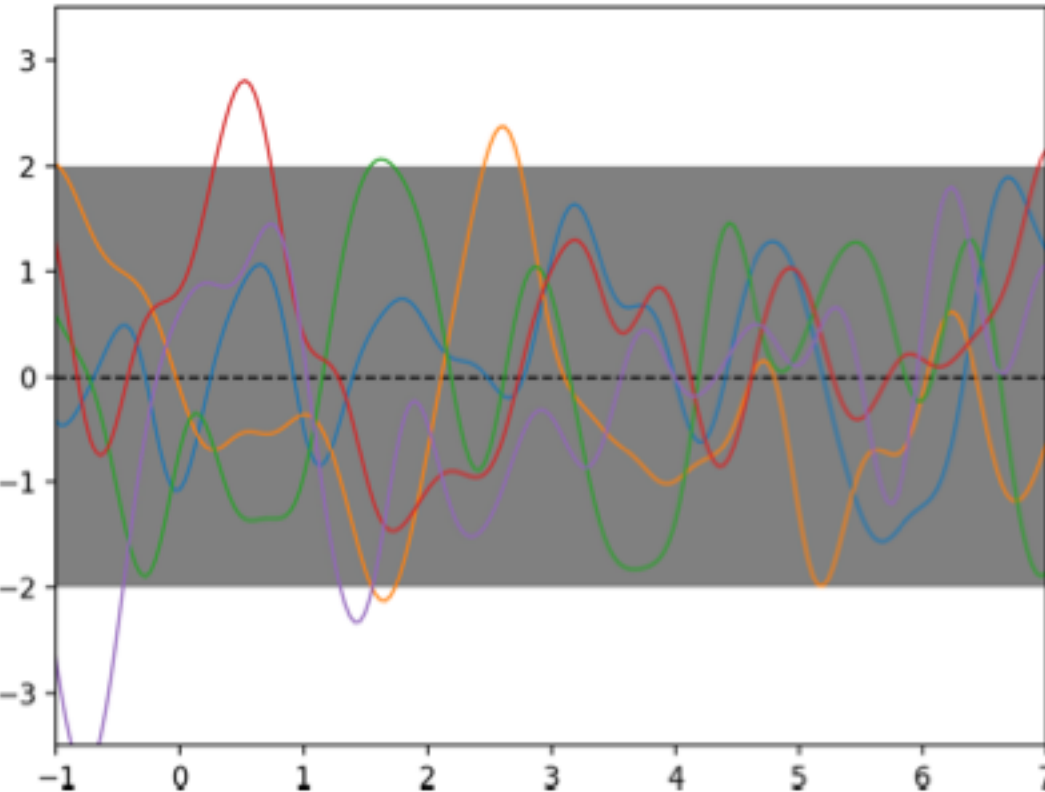
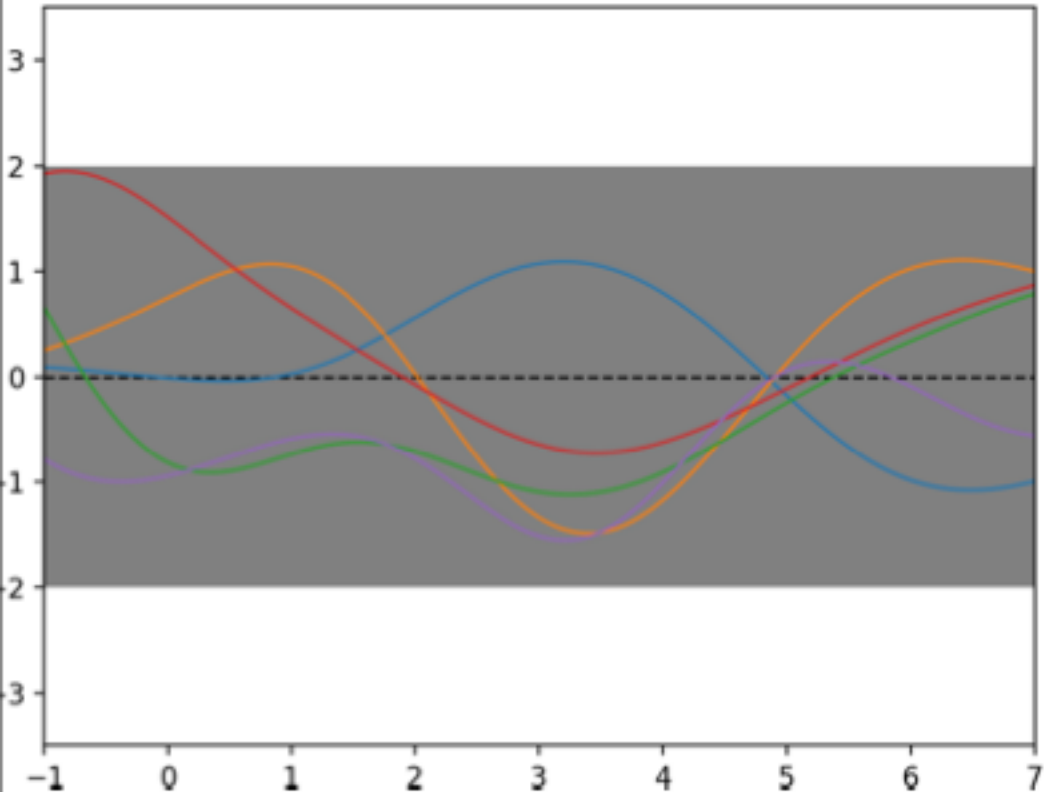


$$\mathcal{L} \equiv (2\pi)^{-\frac{N}{2}} \det|\mathbf{K}|^{-\frac{1}{2}} \exp \left[ -\frac{1}{2} (\mathbf{f} - \bar{\mathbf{f}})^T \mathbf{K}^{-1} (\mathbf{f} - \bar{\mathbf{f}}) \right] \quad \mu(x) = 0 \quad K_{SE}(x, y) = \exp \left[ -\frac{(x - y)^2}{2\ell^2} \right]$$

↖ Likelihood of function values  $\mathbf{f}$  given GP model  $K(x,y)$   
↖ Vector of function values on stencil of points  
↖ Matrix of covariances between stencil points

$\ell = 1.5$

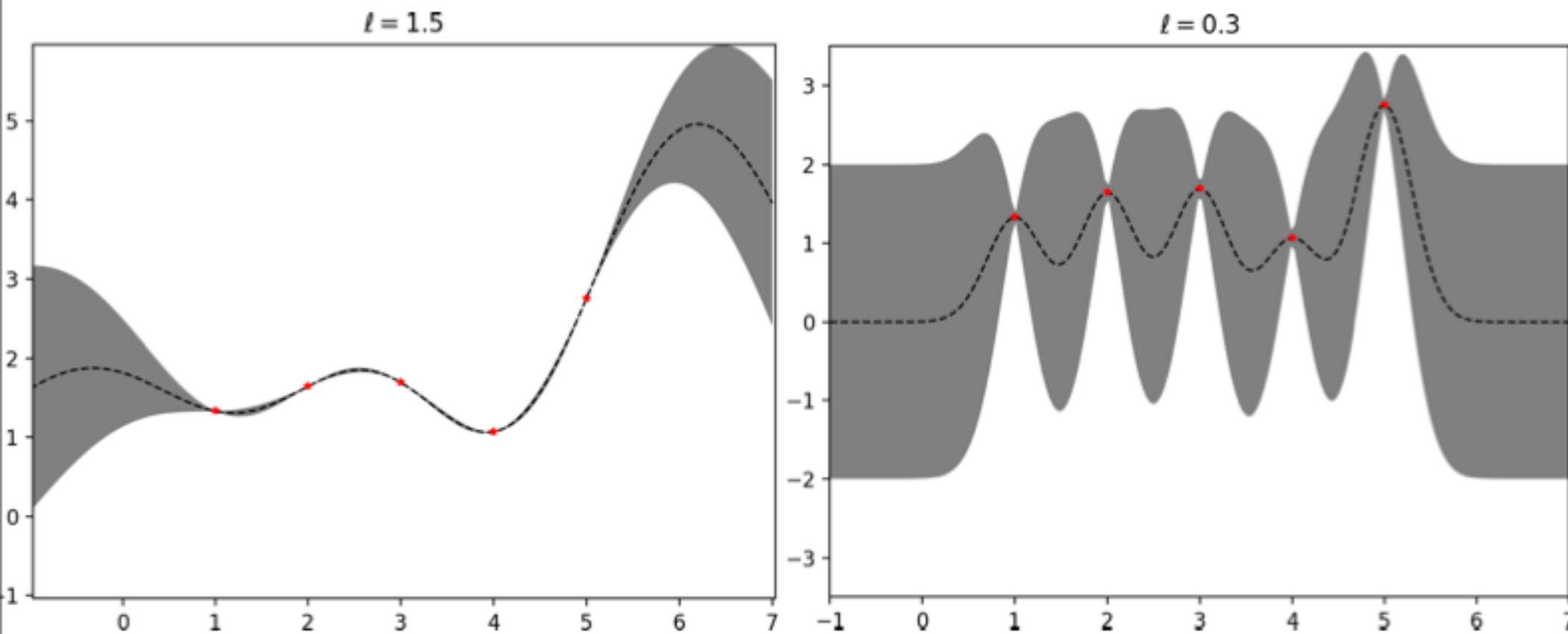
$\ell = 0.3$



$$\tilde{f}_* \equiv \bar{f}(\mathbf{x}_*) + \mathbf{k}_*^T \mathbf{K}^{-1} (\mathbf{f} - \bar{\mathbf{f}}) \quad \mu(x) = 0 \quad K_{SE}(x, y) = \exp \left[ -\frac{(x - y)^2}{2\ell^2} \right]$$

 Covariance between prediction and stencil points

Prediction maximizes joint Gaussian Likelihood



- Need derivative and transverse averaging

$$\frac{1}{\Delta y} \int_{y_{j-1/2}}^{y_{j+1/2}} \frac{\partial f(x, y)}{\partial x} \Big|_{x=x_i} dy$$

- Linear functionals operating on a GP function results in a GP with linearly transformed covariances

$$f(\mathbf{x}_*) \approx \mathbf{k}^T(\mathbf{x}_*, \mathbf{x}_i) \cdot \mathbf{K}^{-1}(\mathbf{x}_i, \mathbf{x}_j) \cdot \mathbf{f}(x_j)$$

Covariance between prediction and stencil points

Covariance between stencil points

$$\int_{y_{j-1/2}}^{y_{j+1/2}} \frac{\partial f(x, y)}{\partial x} \Big|_{x=x_*} dy \approx \mathbf{T}^T(\mathbf{x}_*, \mathbf{x}_i) \cdot \mathbf{K}^{-1}(\mathbf{x}_i, \mathbf{x}_j) \cdot \mathbf{f}(x_j)$$

Covariance between stencil input and linearly transformed output

$$\frac{1}{\Delta y} \int_{y_{j-1/2}}^{y_{j+1/2}} \frac{\partial}{\partial x} \mathbf{k}^T(\mathbf{x}, \mathbf{x}_i) \Big|_{x=x_*} dy$$

● Previously applied to FVM reconstruction and AMR prolongation

S. I. Reeves, D. Lee, A. Reyes, C. Graziani, and P. Tzeferacos, "An application of Gaussian process modeling for high-order accurate adaptive mesh refinement prolongation," *Communications in Applied Mathematics and Computational Science*, vol. 17, no. 1, pp. 1–41, Feb. 2022, doi: [10.2140/cameos.2022.17.1](https://doi.org/10.2140/cameos.2022.17.1).

R. Bourgeois and D. Lee, "GP-MOOD: A positive-preserving high-order finite volume method for hyperbolic conservation laws," *arXiv:2110.08683 [astro-ph, physics:physics]*, Oct. 2021, Accessed: Nov. 08, 2021. [Online]. Available: <http://arxiv.org/abs/2110.08683>

A. Reyes, D. Lee, C. Graziani, and P. Tzeferacos, "A variable high-order shock-capturing finite difference method with GP-WENO," *Journal of Computational Physics*, vol. 381, pp. 189–217, Mar. 2019, doi: [10.1016/j.jcp.2018.12.028](https://doi.org/10.1016/j.jcp.2018.12.028).

A. Reyes, D. Lee, C. Graziani, and P. Tzeferacos, "A New Class of High-Order Methods for Fluid Dynamics Simulations using Gaussian Process Modeling," *Journal of Scientific Computing*, 2016, doi: [10.1007/s10915-017-0625-2](https://doi.org/10.1007/s10915-017-0625-2).

$$f(\mathbf{x}_*) \approx \mathbf{k}^T(\mathbf{x}_*, \mathbf{x}_i) \cdot \mathbf{K}^{-1}(\mathbf{x}_i, \mathbf{x}_j) \cdot \mathbf{f}(x_j)$$

Covariance between prediction and stencil points

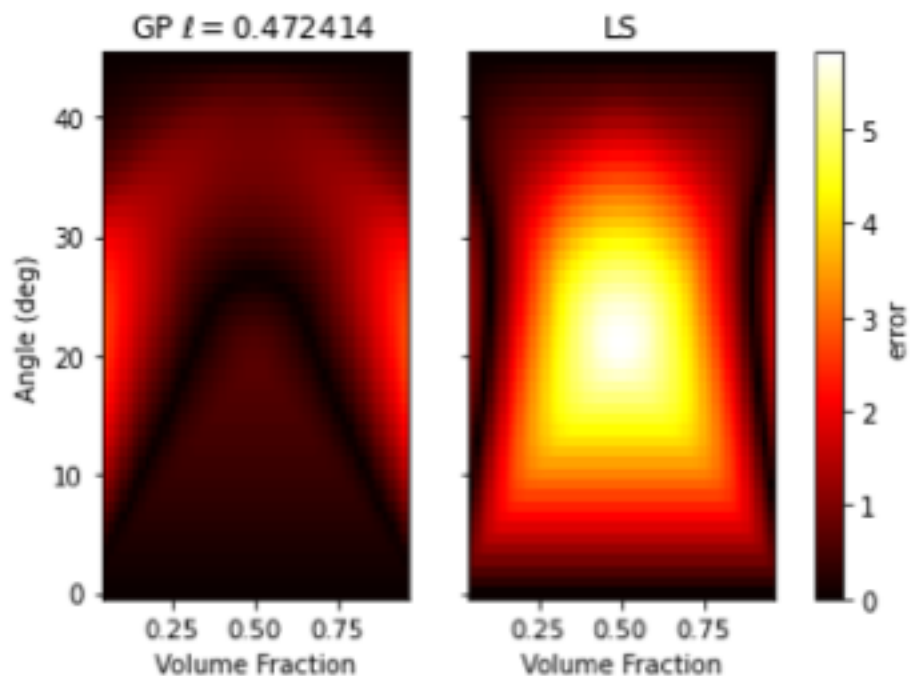
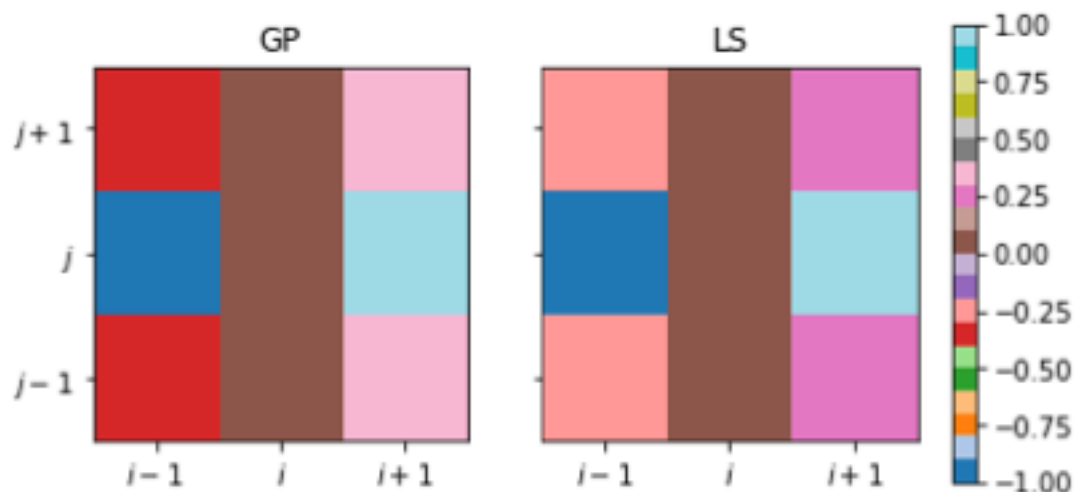
Covariance between stencil points

$$\int_{y_{j-1/2}}^{y_{j+1/2}} \left. \frac{\partial f(x, y)}{\partial x} \right|_{x=x_*} dy \approx \mathbf{T}^T(\mathbf{x}_*, \mathbf{x}_i) \cdot \mathbf{K}^{-1}(\mathbf{x}_i, \mathbf{x}_j) \cdot \mathbf{f}(x_j)$$

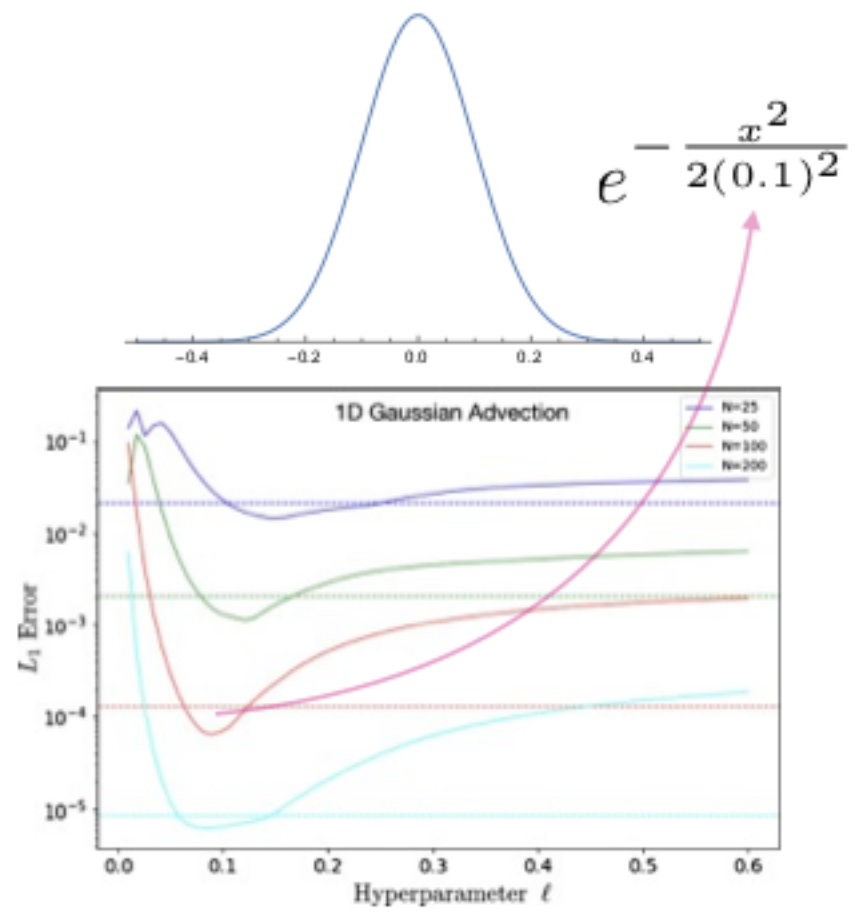
Covariance between stencil input and linearly transformed output

$$\frac{1}{\Delta y} \int_{y_{j-1/2}}^{y_{j+1/2}} \left. \frac{\partial}{\partial x} \mathbf{k}^T(\mathbf{x}, \mathbf{x}_i) \right|_{x=x_*} dy$$

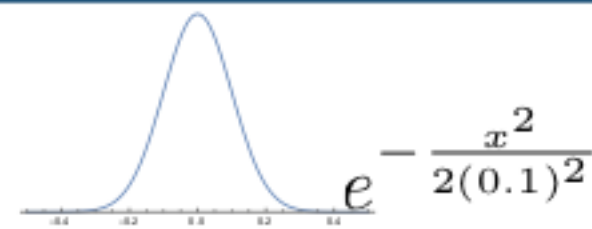
- GP Stencil weighs more the diagonal elements
- GP calculation of interface normal is able to achieve much lower errors on the same stencil as least-squares Youngs method



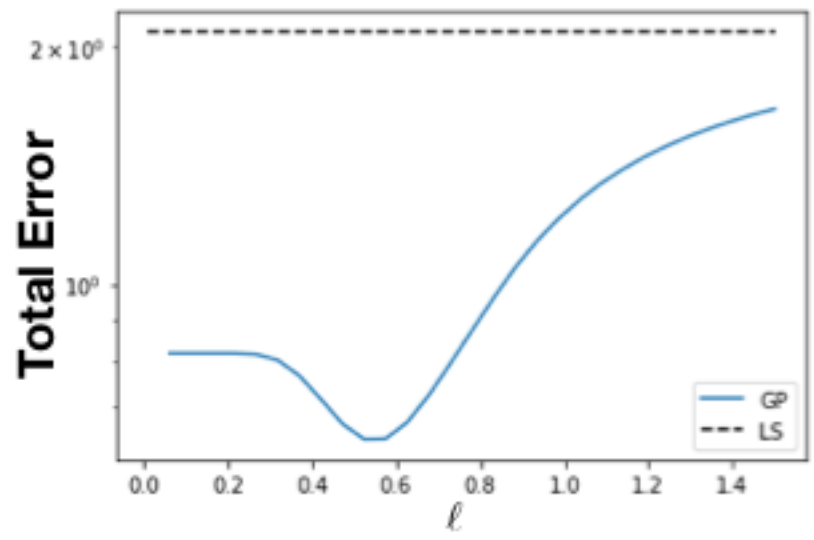
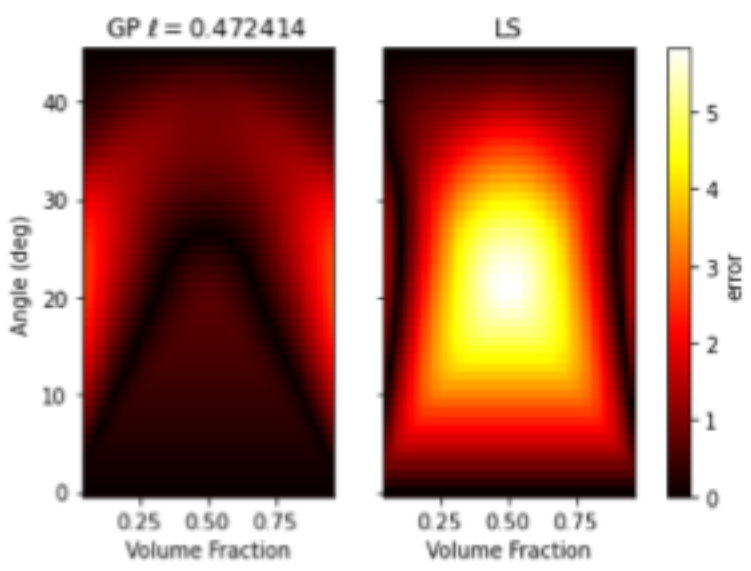
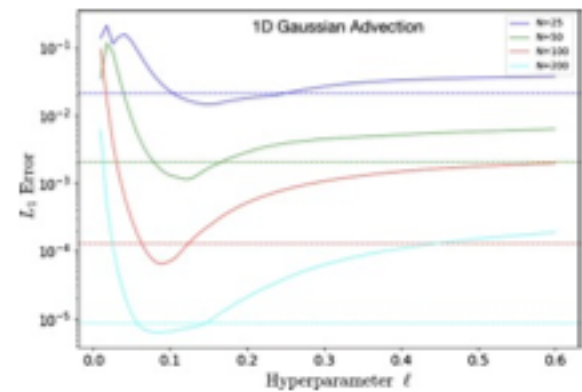
- How to choose a length scale?
- Characteristic to variation in the problem



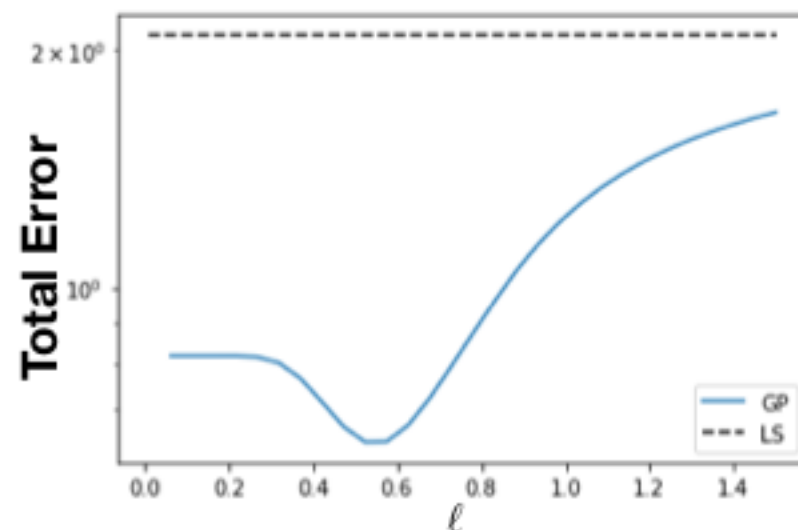




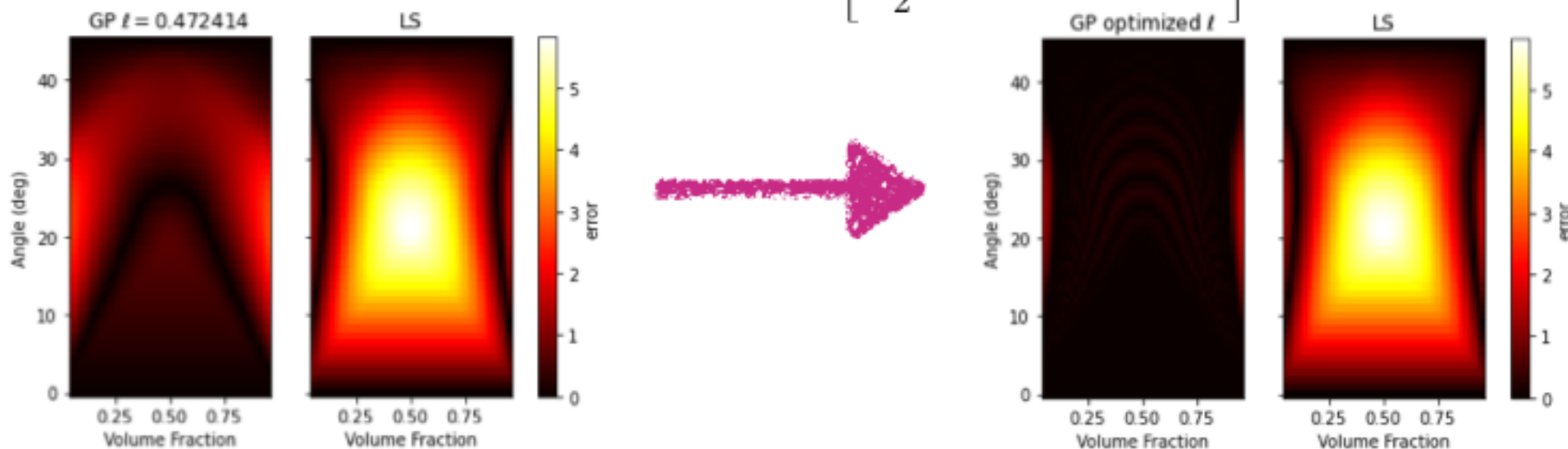
- How to choose a length scale?
  - Characteristic to variation in the problem
  - Can minimize error over all possible linear interfaces (volume fraction and angle)



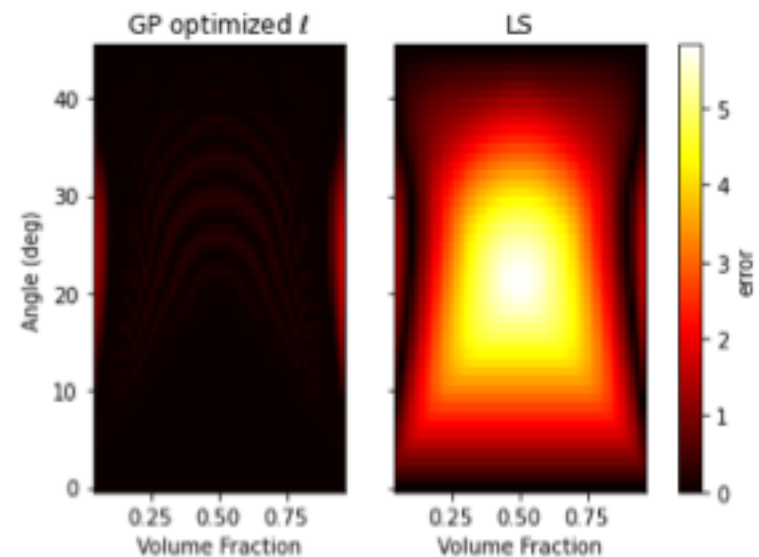
- How to choose a length scale?
  - Characteristic to variation in the problem
  - Can minimize error over all possible linear interfaces (volume fraction and angle)
  - Look for minimum error depending on data



$$\mathcal{L} \equiv (2\pi)^{-\frac{N}{2}} \det|\mathbf{K}|^{-\frac{1}{2}} \exp \left[ -\frac{1}{2} (\mathbf{f} - \bar{\mathbf{f}})^T \mathbf{K}^{-1} (\mathbf{f} - \bar{\mathbf{f}}) \right]$$



- Volume of Fluid (VOF) methods combine conservation with sharp interface representation
  - Computationally efficient interface reconstruction algorithms that generalize to 3D can fail, even for simple linear interfaces
- non-parametric Gaussian process function regression allows one to more accurately reconstruct interfaces, with the same computational cost
  - Going further, GP hyperparameters may be locally tuned to minimize errors



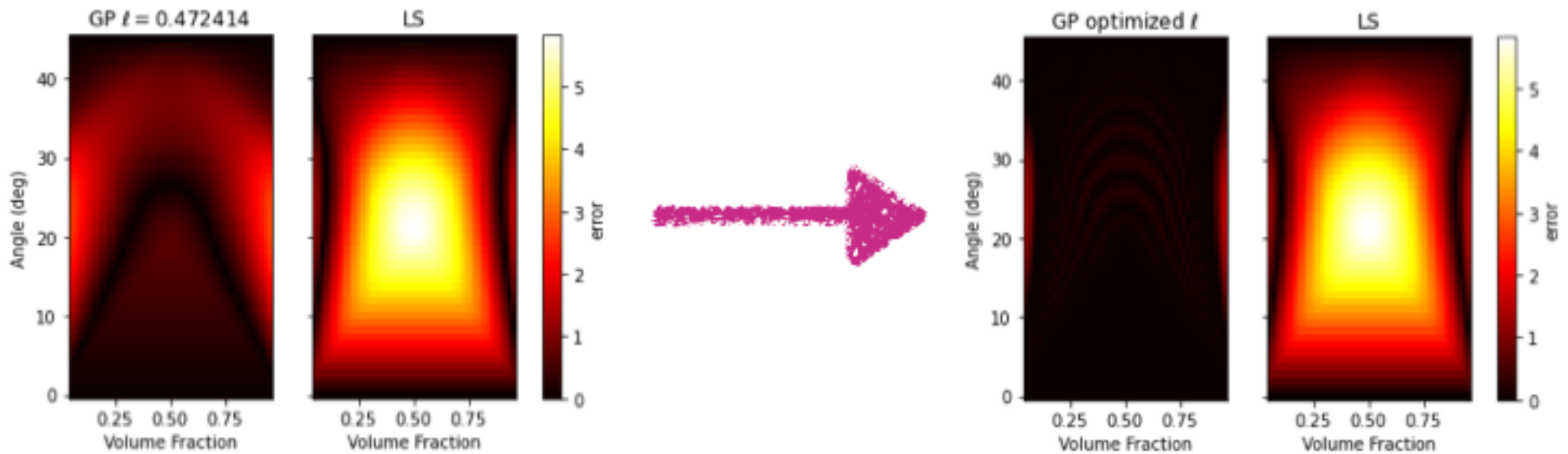
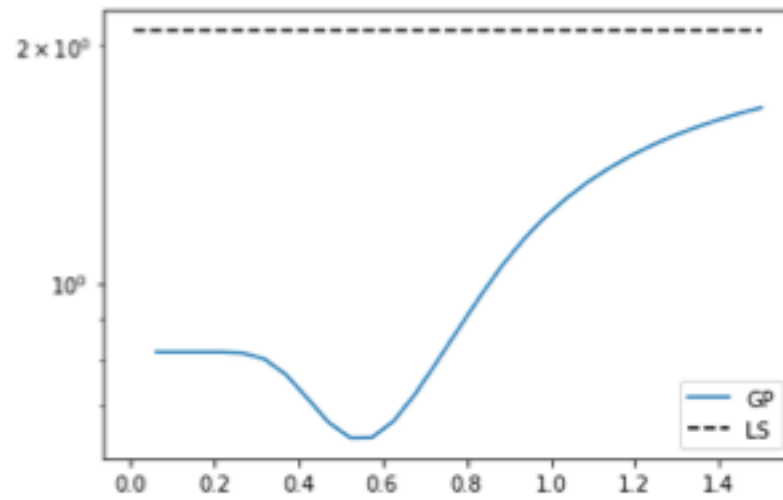
# Backup Slides



UNIVERSITY OF  
ROCHESTER



# Optimization



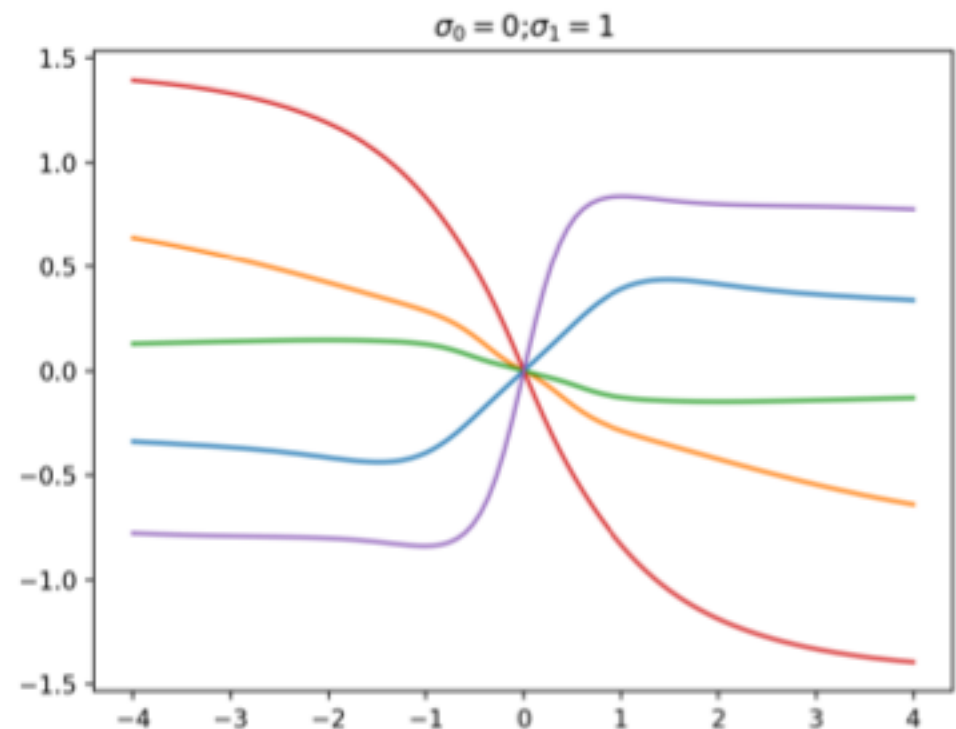
- Neural Network covariance function

- Produces functions that are **superpositions of error functions**

$$\text{erf}(u_0 + u_1 x)$$

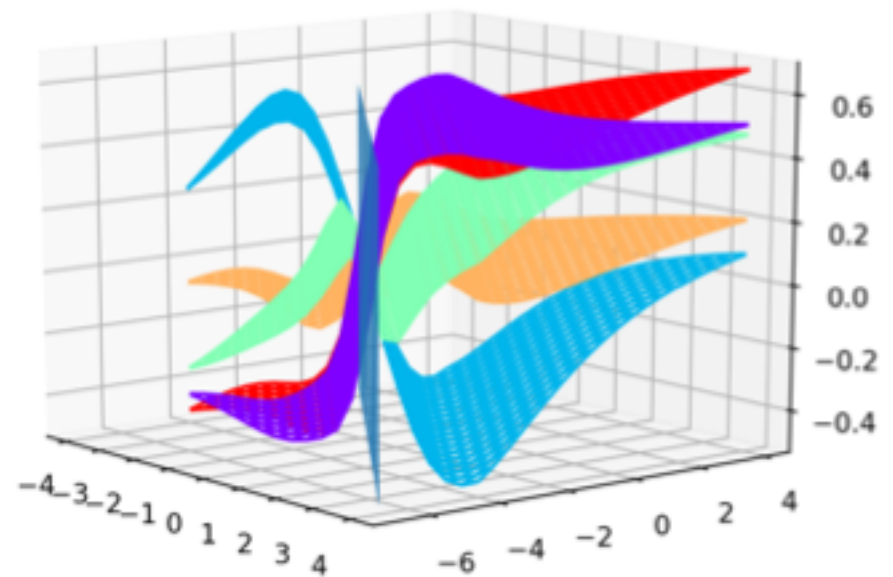
$$u_0 \sim \mathcal{N}(0, \sigma_0^2) \quad u_1 \sim \mathcal{N}(0, \sigma_1^2)$$

$$k_{\text{NN}}(x, y) = \frac{2}{\pi} \sin^{-1} \left( \frac{2(\sigma_0 + \sigma_1 xy)}{\sqrt{(1 + 2(\sigma_0 + \sigma_1 x^2))(1 + 2(\sigma_0 + \sigma_1 y^2))}} \right)$$



- Convolution of a GP kernel with another function produces a valid kernel
- Can use any parametrized curve
- Use GP optimization to “learn” curve parameters, such as normal and line constant

$$k'(x, y) = k(\phi(x), \phi(y))$$



Random GP samples from NN covariance with

$$\phi(\mathbf{x}) = \frac{\mathbf{n} \cdot \mathbf{x} + \rho}{|\mathbf{x}|}$$

$$\mathcal{L} \equiv (2\pi)^{-\frac{N}{2}} \det|\mathbf{K}|^{-\frac{1}{2}} \exp \left[ -\frac{1}{2} (\mathbf{f} - \bar{\mathbf{f}})^T \mathbf{K}^{-1} (\mathbf{f} - \bar{\mathbf{f}}) \right]$$



- Mark cells that are either mixed or will potentially become mixed
- Update single fluid states just as before
  - Get volume flux ( $u^*$ ) at each interface
- Reconstruct linear interfaces using  $f^\alpha$  &  $\nabla f_i^\alpha$

$$\mathbf{n} \cdot \mathbf{x} + \rho = 0$$

